Pancreatic Bicarbonate Secretion Involves Two Proton Pumps*[S]

Ivana Novak[‡1], **Jing Wang**[‡], **Katrine L. Henriksen**[‡2], **Kristian A. Haanes**[‡], **Simon Krabbe**[‡], **Roland Nitschke**[§3], **and Susanne E. Hede**[‡]

From the [‡]*Department of Biology, August Krogh Building, University of Copenhagen, Universitetsparken 13, DK-2100 Copenhagen, Denmark and the* [§]*Life Imaging Center for Biological Analysis and Center for Biological Signaling Studies, Albert-Ludwigs-University, D-79104 Freiburg, Germany*

Pancreas secretes fluid rich in digestive enzymes and bicarbonate. The alkaline secretion is important in buffering of acid chyme entering duodenum and for activation of enzymes. This secretion is formed in pancreatic ducts, and studies to date show that plasma membranes of duct epithelium express H^+/HCO_3^- transporters, which depend on gradients created by the Na^+/K^+-ATPase. However, the model cannot fully account for high-bicarbonate concentrations, and other active transporters, *i.e.* pumps, have not been explored. Here we show that pancreatic ducts express functional gastric and non-gastric H^+-K^+-ATPases. We measured intracellular pH and secretion in small ducts isolated from rat pancreas and showed their sensitivity to H^+-K^+ pump inhibitors and ion substitutions. Gastric and non-gastric H^+-K^+ pumps were demonstrated on RNA and protein levels, and pumps were localized to the plasma membranes of pancreatic ducts. Quantitative analysis of H^+/HCO_3^- and fluid transport shows that the H^+-K^+ pumps can contribute to pancreatic secretion in several species. Our results call for revision of the bicarbonate transport physiology in pancreas, and most likely other epithelia. Furthermore, because pancreatic ducts play a central role in several pancreatic diseases, it is of high relevance to understand the role of H^+-K^+ pumps in pathophysiology.

Transport of acids and bases over cell membranes is essential for the function of every cell in the body. Some organs maintain body acid/base homeostasis, while others utilize acid/base transport for special purposes, such as digestion, and transport significant quantities of H^+ and HCO_3^-. Pancreatic ducts secrete a HCO_3^--rich fluid (40–150 mM) that conveys an enzyme-rich fluid produced by pancreatic acini. How is such secretion formed? Most simply, one can envisage that transepithelial HCO_3^- secretion can occur by moving HCO_3^- from serosa to lumen and/or by H^+ transport in the opposite direction. From first electrophysiological and intracellular pH studies on isolated rat pancreatic ducts, the working cellular model for bicarbonate transport was proposed and later extended to account for HCO_3^- transport in pancreas of other species, and also in other HCO_3^--transporting epithelia (1–3). Basically, on the basolateral membrane the model includes transporters that would lead to accumulation of cellular HCO_3^-, a Na^+/H^+ exchanger (NHE)[4] and a Na^+-HCO_3^- cotransporter (NBC) that belongs to the SLC4 bicarbonate transporter gene family. On the luminal membrane HCO_3^- efflux would occur via Cl^-/HCO_3^- anion exchanger (AE) belonging to the sulfate permease family, *e.g.* SLC26A6 (3). Following hormonal or neural stimulation, the whole process would be initiated by opening of luminal Cl^- channels: the cystic fibrosis transmembrane conductance regulator (CFTR) Cl^- channels, which may have some HCO_3^- permeability; or the Ca^{2+}-activated Cl^- channels. The membrane potential and driving force on anion secretion would be provided by K^+ channels (4). The main feature of this model is that H^+/HCO_3^- transport is secondary active and relies on ion gradients created by the primary active transporter, the Na^+/K^+-ATPase. Nevertheless, given the ion selectivity, electrochemical gradients and unusual regulation of CFTR and Cl^-/HCO_3^- exchange by extracellular HCO_3^- and Cl^-, it is unclear how pancreatic ducts can secrete more than 80–100 mmol/liter HCO_3^- to the lumen (3). Several earlier studies on pancreatic ducts searched for a primary active transporter, the vacuolar H^+ pump, but evidence at the molecular level is missing and functional data on this issue are contradictory (5–7).

In the present study we addressed the question of whether pancreatic ducts possess another functional H^+ pump, namely an H^+-K^+-ATPase, which could participate in H^+/HCO_3^- transport. The H^+-K^+-ATPases belong to the large family of P-type ATPases, and each pump is made up of two catalytic α-subunits and two regulatory β-subunits. The α-subunits of H^+-K^+-ATPase are classified into two groups, gastric and non-gastric (latter also called colonic), coded by the *ATP4A* gene and *ATP12A* gene (latter denoted also *ATP1AL1*). There is 60–65% homology between the α-sub-

units of these pumps and the closest relative, the Na^+/K^+-ATPase. The gastric α-subunit (HKα1) assembles with the gastric β-subunit (HKβ); the non-gastric α-subunit (HKα2) can also assemble with the gastric β-subunit, although it can also borrow the β1-subunit of the Na^+/K^+-ATPase or assemble with different β-subunits and other associating proteins (8–13). The gastric pump is able to create large H^+ (and HCO_3^-) gradients and it has a clear physiological function in HCl secretion by parietal cells of the stomach. In kidney distal nephrons and cochlea, the pump may be responsible for constitutive H^+ secretion and K^+ absorption, and K^+ recirculation, respectively (14, 15). Many other epithelial tissues, such as colon, kidney, skin, placenta, and prostate, express non-gastric H^+-K^+ pumps. These can contribute to H^+ secretion and K^+ absorption, but this is usually associated with conditions of disturbed acid-base or K^+ and Na^+ homeostasis rather than the "normal" physiological situation (9, 14, 16).

EXPERIMENTAL PROCEDURES

Solutions and Chemicals—Control bathing solutions containing bicarbonate had the following composition (in mmol/liter): Na^+ 145, Cl^- 125, HCO_3^- 25, K^+ 4, Ca^{2+} 1.5, Mg^{2+} 1, phosphate 2, glucose 5; they were equilibrated with 5% CO_2 in O_2; pH was 7.4. In HCO_3^--free solutions $NaHCO_3$ was replaced with NaCl or sodium gluconate and 10 mM HEPES was used as a buffer. For ammonium pulses 20 mmol/liter Na^+ was replaced with NH_4^+. In Na^+ and K^+-free solutions, N-methyl-D-glucamide was used for replacement. The following inhibitors were used: 4′-4′-diisothiocyanate-dihydro-stilbebe-2,2′-disulfonacid (H_2DIDS, 0.5 mM), omeprazole (10 μM), and SCH-28080 (100 μM); and prepared according to the instructions (Sigma, Denmark). The primary antibodies were: Calbiochem 119100 (HK12.18, anti HKα1 monoclonal); Calbiochem 119101 (anti HKα1 polyclonal, against C-terminal), Chemicon AB 1679 (anti HKα1 polyclonal, against N-terminal), or Sigma A-274 (2G11, anti HKβ, monoclonal). Rat non-gastric HKα2 antibody (C384-M79) raised against (Glu^{528}–Met^{555}) (17) was kindly donated by J. J. H. H. M. De Pont and H. G. P. Swarts. Secondary antibodies were conjugated to Alexa dyes or Cy3) (Invitrogen, Jackson ImmunoResearch).

Preparation of Ducts—Protocols involving handling of animals were approved by the Danish Animal Experiment Inspectorate (*Dyreforsøgstilsynet*). Wistar rats were killed by cervical dislocation and pancreas was removed. Subsequently, collagenase digestion and dissection was carried out according to previously published method (18). In a dissection microscope ducts were identified from their appearance and relation to other structures, similar to a morphological study (19). After transfer to a higher resolution microscope, ducts were measured and epithelium type confirmed. For this study we used small ducts, some of the intercalated type (closest to acini) and mostly small intralobular duct fragments (Fig. 1*A*). Larger ducts between pancreatic lobules, interlobular ducts, were not used. Fig. 1*B* shows the size distribution (outer diameter) of the ducts used in this study; their length was 200–500 μm. Ducts were placed in an experimental chamber on an inverted microscope and used for pH$_i$ measurements or for secretion studies. Small duct fragments were held by holding

pipettes, but could not be perfused, although we can perfuse larger microdissected ducts (20).

pH$_i$ Measurements—Detailed methods for pH$_i$ measurement in pancreatic ducts are described elsewhere (21). Briefly, pancreatic ducts were loaded with BCECF/AM (2 μM), for 20–30 min; thereafter they were kept at 37 °C in perfused experimental chamber. Both the luminal and the basolateral sides were accessible to the bathing solution. Intracellular pH (pH$_i$) was estimated from changes in the fluorescence emission (at 510 nm) from 15–20 cells after excitation at 488 and 436 nm. Signals were calibrated *in situ* with 10 μM nigericin in high K^+ buffers, and the fluorescence ratios and pH$_i$ were fitted to a calibration curve. A standard method of ammonium pre-pulse was used to study H^+/HCO_3^- transport. Tissues were exposed to ammonium pulses (2–3 min), then ammonium was removed, and pH$_i$ recovery rates from acidosis were determined from the initial slopes of pH$_i$ changes and expressed as *dpH/dt* (*i.e.* pH units/minute). Also *dpH/dt* was converted to the transmembrane H^+ flux, $J(H)^+$ (in mmol·liter·cell water^{-1}·min^{-1}), taking into account appropriate buffering capacities at given pH$_i$, as we described earlier (21).

Measurements of Secretion in Isolated Ducts—Pancreatic ducts were placed in chambers containing bicarbonate buffer gassed with humidified 5% CO_2 in O_2 and temperature was 37 °C. Ducts were held by one holding, occluding pipette. Dextran Texas Red 10,000 MW (25 μg/ml) was added, and ducts were allowed to rest about 30 min. The fluorophore was excited at 568 nm, and emission was monitored at 600–650 nm every 20 s in Leica TCS NT/SP CLSM microscope. First, images were collected from non-stimulated duct. Subsequently, ducts were exposed to secretin ± inhibitors (Omeprazole and SCH-28080) for 10–20 min. After a wash and rest of ~20 min, the same ducts were subjected to the second stimulation protocol. A region of interest, ROI (50–200 μm), was drawn on a part of the duct that was not moving or did not appear leaky. Image analysis was performed in Meta-Morph 5 using integrated morphometry analysis. Images were first converted to monochrome, equalized, aligned, thresholded, and converted to binary images. Area within ROI in the lumen was calculated and used for the volume (V) estimation, assuming that the duct segment was a cylinder. The volume was calculated for each frame and for comparison between different ducts it was expressed in relation to the first frame as V$_{rel}$. The area of the duct epithelium (E) facing the lumen was estimated, assuming that the duct lumen increased in radius, length was delimited by ROI. Finally, the secretory rate (Jv) per epithelium area was calculated from the following equation using the initial area for the calculation: $Jv = (dV_{rel}/dt)/E$.

RT-PCR and Western Blot Analysis—RNA from whole pancreatic tissue, pancreatic ducts, colon, and stomach was isolated using TRIzol reagent (Invitrogen), and method was optimized similar to published protocols (22). The RT-PCR reactions were done with OneStep reaction kit (Qiagen) using designed primers (Table 1). RNA was also extracted from single intercalated/intralobular pancreatic ducts pooled in lots of 3 per vial and checked for contamination using specific prim-

ers for thrombin and amylase according to the previously published method (18). Only non-contaminated RNA was used for further analysis. Because this RNA was limited, an additional PCR reaction was performed on RT-PCR products with specific nested PCR primers (Table 1). Primers were designed using VectorNTI software (Invitrogen) and identity of all products was confirmed by sequencing (MWG Biotech, Ebersberg, Germany).

For protein isolation, pancreas, and other organs were excised, cut into small pieces, and washed with ice-cold PBS. Tissues were homogenized in $3\sim5$ ml homogenization buffer with SigmaFAST protease inhibitor and centrifuged at $15,000 \times g$ for 15 min at 4 °C. The supernatant was centrifuged at $190,000 \times g$ for 1 h at 4 °C. The resulting pellet was washed with 250 mM KBr and re-centrifuged to pellet membranes, which were then washed in 100 mM Na_2CO_3 at pH 11 and then centrifuged for a final time. The microsomes were dissolved in lysis buffer. All solutions contained $1\times$ Sigma protease inhibitor (S-8820). Protein digestion due to endogenous pancreatic proteases is a common problem. To reduce the amount of digestive enzymes, we optimized the method as follows. Pancreas pieces were homogenized in ice-cold SME buffer (250 mM sucrose, 25 mM MES, 2 mM EGTA, pH 6). Our new method includes a double centrifugation, which was established to remove the fraction containing zymogen granules (23). The first pellet after the $250 \times g$ centrifugation and the second supernatant after the $1,400 \times g$ centrifugation were mixed and re-homogenized. Then the similar procedure for preparing the microsomes was followed as given above. Protein samples were loaded on 10% or $4\sim12$% polyacrylamide gels (Invitrogen), separated by electrophoresis, and blotted to PVDF membranes (Invitrogen). Membranes were blocked overnight at 4 °C or 1 h at room temperature and incubated for 2 h at room temperature or overnight at 4 °C with primary antibodies recognizing the gastric HKα1 (Calbiochem 119101, 1:1,000), gastric HKβ (Sigma A274, 1:4,000), or non-gastric HKα2 (1:1,000). Blots were incubated with appropriate HRP-conjugated antibodies (DAKO, diluted 1:2,500), developed with ECL (Amersham Biosciences) and visualized by exposure on films (General Electrics).

Immunocytochemistry—Paraffin or cryosections from pancreas, colon, and stomach were prepared from control rats, and in some cases rats were previously stimulated with secretin as published (24). Tissues were fixed in methanol at -20 °C for 5 min, or in 4% paraformaldehyde PBS for 15 min, and the latter were permeabilized with 0.1% Triton X-100 and 1% BSA in PBS for $10-12$ min. Samples were blocked for 30 min in 3% BSA in PBS and incubated overnight at 4 °C with primary antibodies against various HK subunits (see above) in dilutions 1:300 to 1:100. Secondary antibodies conjugated to Alexa dyes or Cy3 (1:400) (Invitrogen, Jackson ImmunoResearch) were added for 45 min. In control samples done with every run, primary or secondary antibodies were omitted. Nuclei were stained with DAPI ($300-400$ nM) for 5 min. Samples were mounted with 2% *n*-propylgallat and 90% glycerol. Fluorescence was examined in a Leica TCS NT/SP CLSM with 40×1.2 NA or 100×1.4 NA oil objectives. Images and overlays were analyzed in Leica software or in MetaMorph 5 and
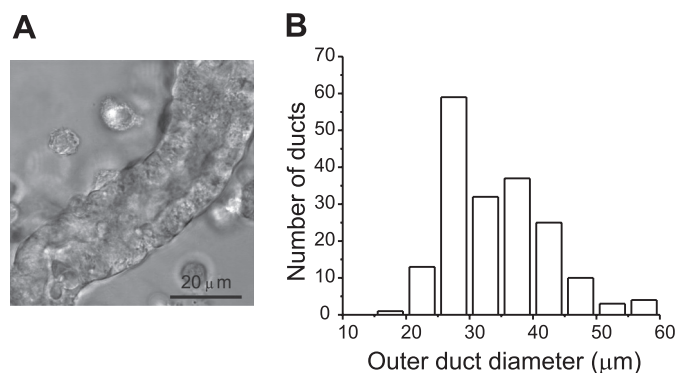

FIGURE 1. **Isolated rat pancreatic ducts.** *A*, an example of a small intralobular duct used for the study. *B*, diagram shows the frequency distribution of outer diameter of pancreatic ducts used in the present study.
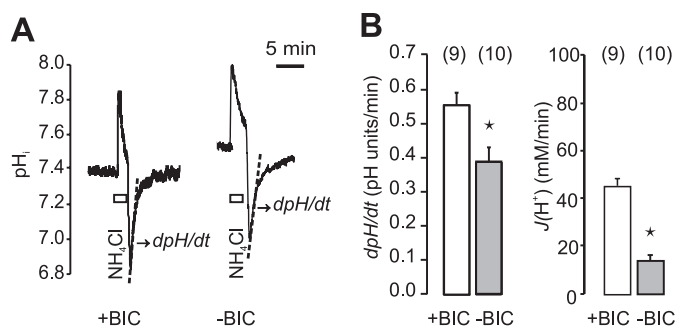

FIGURE 2. **Recovery of pH$_i$ from acidosis in the presence and absence of HCO$_3^-$/CO$_2$ in the buffers.** *A*, an example of a pH$_i$ measurement in a duct challenged with a control ammonium pulse in a buffer containing HCO$_3^-$/CO$_2$ (+BIC) and later without HCO$_3^-$/CO$_2$ (−BIC). *Dotted lines* show the initial slope of the pH$_i$ recovery from acidosis, *i.e. dpH/dt*. *B*, summary of recovery rates expressed as *dpH/dt* and converted to proton efflux *J*(H$^+$) for pancreatic ducts bathed in +BIC and -BIC solutions ($n = 9$ and 10, respectively). *Asterisks* indicate that the *dpH/dt* and *J*(H$^+$) values are significantly different in +BIC and −BIC solutions ($p < 0.05$, unpaired *t* test).

exported as TIFF files to CorelDraw for composite picture. Except for cropping, no image manipulation was used.

Statistics—Data are presented as original recordings and summaries showing the mean values $\pm$ S.E. Control and test measurements were made within the same ducts as far as possible, and *n* refers to measurements on different ducts. Student's *t* test, paired, and in some cases unpaired, was applied. $p < 0.05$ was accepted as significant and denoted with *asterisks*. Data were analyzed in Origin (Microcal Software, Inc).

RESULTS

Duct pH$_i$ Is Regulated by Several H⁺/HCO$_3^-$ Transporters Including H⁺-K⁺ Pumps—To determine ion transporters regulating intracellular pH (pH$_i$) and transmembrane H⁺/HCO$_3^-$ transport, we isolated single ducts from rat pancreas and stimulated them with secretin. We used the smallest pancreatic ducts (intercalated and intralobular) (Fig. 1), which are rich in carbonic anhydrase, CFTR and aquaporins (25–28), and considered the most likely site of HCO$_3^-$ transport. A common protocol to study HCO$_3^-$/H⁺ transport is to monitor the recovery of pH$_i$ following an acid load. This is achieved by pre-pulse with an ammonium buffer (NH$_4^+$/NH$_3$), then upon its removal pH$_i$ falls rapidly due to excess of intracellular H⁺ left after diffusion of NH$_3$ out of cells (Fig. 2*A*). Cells then rapidly regulate pH$_i$ to control levels either by H⁺ export or
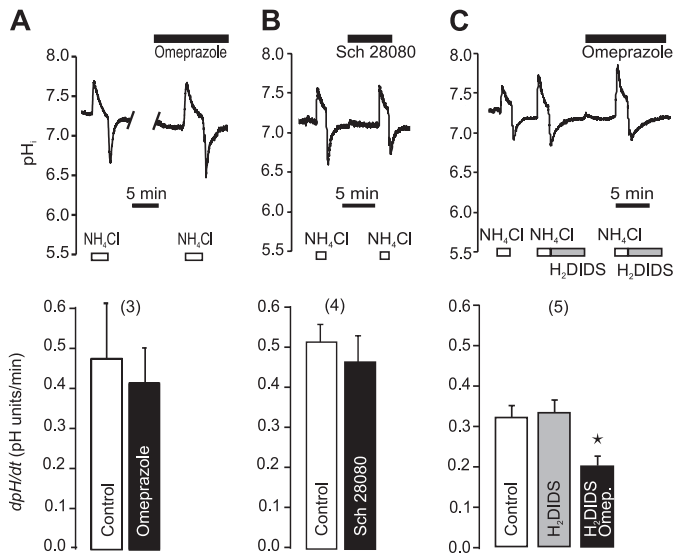
FIGURE 3. **Effect of H^+-K^+ pump inhibitors on recovery of pH_i from acidosis in physiological HCO_3^-/CO_2 buffers.** Top figures show original pH_i recordings in single pancreatic ducts, where the rate of recovery from acid load (NH_4Cl removal) was challenged by different inhibitors. Bottom figures show the respective summaries. The following inhibitors were used: *A*, omeprazole (10 μM); *B*, SCH-28080 (0.1 mM); and *C*, omeprazole (10 μM) and H_2DIDS (0.5 mM). All ducts were stimulated with secretin (1 nM), and buffers contained HCO_3^-/CO_2. Bars show paired measurements as means ± S.E., *n* are number of experiments, and *asterisks* indicates $p < 0.05$.

FIGURE 4. **Removal of extracellular Na^+ (in $-$BIC solution) inhibits most but not all pH_i recovery from acidosis.** *A*, example of a pH_i measurement in a duct challenged with a control ammonium pulse and later with an ammonium pulse where Na^+ was removed during the first 5 min of the recovery period. When Na^+ was added back to the bathing solution, the duct pH_i recovered completely. *B*, comparison of pH_i recovery from ammonium-induced acidosis during control conditions in -BIC (*C*) and in Na^+-free conditions (0 Na^+). *Asterisk* indicates $p < 0.05$. *C*, shows *dpH/dt* as a function of the pH_i value from which the ducts started the pH_i recovery after an ammonium pulse in controls and Na^+-free conditions. In the Na^+-free solutions the recovery rate appears to depend on the extent of acidosis. Although the extreme acidic pH_i values may not be accurately estimated with the BCECF fluorophore, it is clear that in the range of pH_i values, common for the two conditions (*i.e.* pH_i 6.6–7.0), the pH_i recovery was slower in the absence of Na^+. All ducts were stimulated with secretin (1 nM).

HCO_3^- import, the latter if extracellular HCO_3^-/CO_2 buffer is provided. This transport can be monitored as *dpH/dt* and this can be converted to the transmembrane flux of H^+, or HCO_3^- (see "Experimental Procedures"). In a physiological HCO_3^-/CO_2 buffer the flux of H^+ or HCO_3^- was 44.36 ± 3.64 mM/min, and in the HCO_3^-/CO_2-free buffer it was 16.74 ± 1.78 mM/min ($n = 9,10$) (Fig. 2). These experiments show that the pH_i recovery was significantly higher in the presence of extracellular HCO_3^-/CO_2 buffer, probably as several transporters contributed to the recovery (see below).

In the following series of experiments on the secretin-stimulated ducts, we tested the effect of H^+-K^+ pump inhibitors (Fig. 3). In physiological buffers, omeprazole (the gastric H^+-K^+ pump inhibitor) had no significant effect on pH_i recovery (Fig. 3*A*). Similarly, SCH-28080 that inhibits the gastric but also non-gastric H^+-K^+ pumps at high concentrations (11, 17), also had no effect on pH_i recovery (Fig. 3*B*). Nevertheless, in epithelial cells transporting H^+ or HCO_3^- across the plasma membranes, one might expect that pH_i would be regulated by several transport systems. We therefore inhibited Cl^-/HCO_3^- exchange and Na^+-HCO_3^- cotransport by H_2DIDS (Fig. 3*C*). Omeprazole now reduced pH_i recovery by 39% ($n = 5$), thus indicating functional H^+-K^+ pumps. Following this reasoning, we eliminated participation of Na^+-dependent and HCO_3^--dependent transporters, such as NHE, NBC, and AE, by simply removing extracellular Na^+ and HCO_3^-/CO_2 buffer (Fig. 4). The ability of stimulated ducts to recover from the experimental acid-load was reduced more than 4-fold in Na^+-free solutions (Fig. 4*B*). Similar ranges of pH_i values were taken into account for control and Na^+-free experiments (Fig. 4*C*). Most importantly, there was a small but significant pH_i recovery even in the absence of
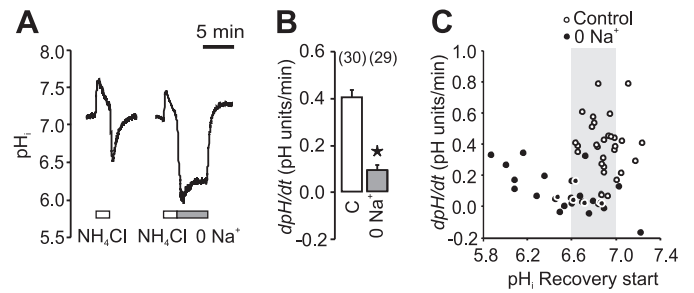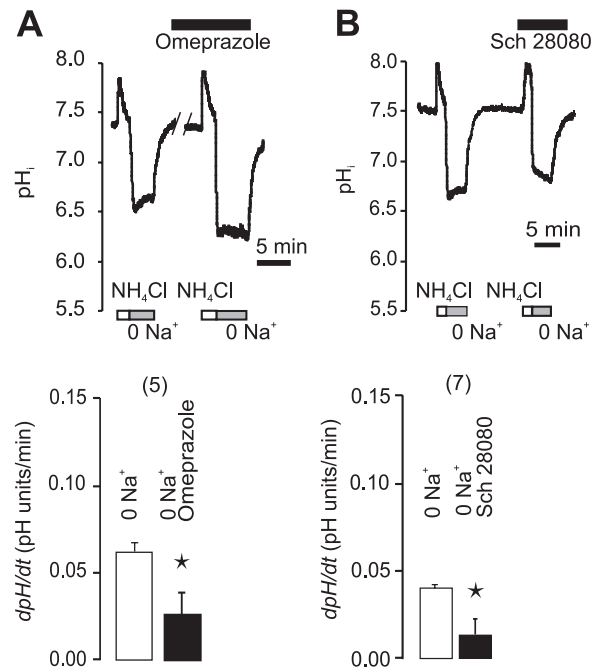

FIGURE 5. **Omeprazole and SCH-28080 inhibits Na^+-independent pH_i recovery.** Experiments were performed in the absence of extracellular HCO_3^-/CO_2, in addition Na^+ was removed as indicated by the *bars*. Ducts were stimulated with secretin (1 nM), as in all other experiments. *A*, example of a pH_i measurement in a duct challenged with an ammonium pulse, where Na^+ was removed during the first 5 min of recovery. After about 10 min, the same maneuver was repeated in the presence of omeprazole (10 μM) in the same duct. Summary data for these experiments are shown in the *bottom* bar graph. *B*, similar experiments were performed on with SCH-28080 and original pH_i response, and summary data are shown.

extracellular Na^+. Therefore, we tested the effect of H^+-K^+ pump inhibitors under these conditions (Fig. 5). Now, both omeprazole and SCH-28080 inhibited 56 and 69% of Na^+-independent pH_i recovery (Fig. 5, *A* and *B*). To further verify the presence of the H^+-K^+-ATPase, we tested the dependence of pH_i recovery on extracellular K^+ and results are shown in Fig. 6*A*. This maneuver is often used for testing of
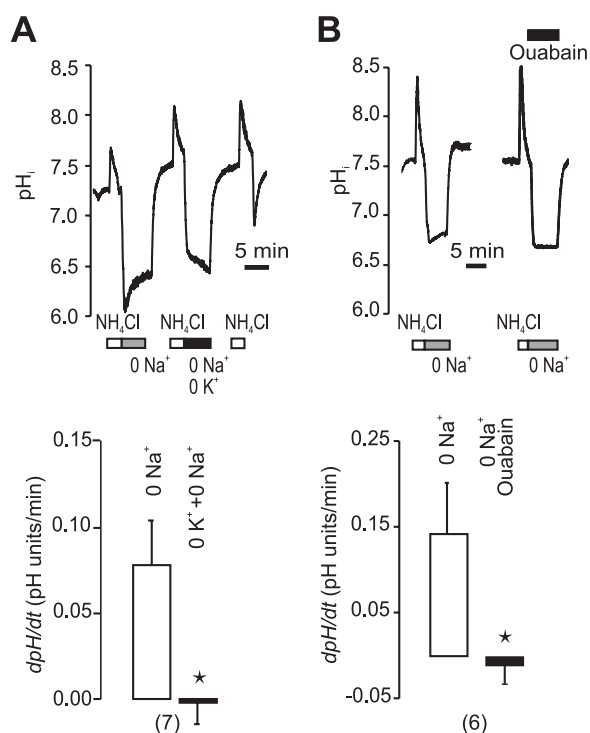
FIGURE 6. **Effect of removal of extracellular K$^+$ and ouabain.** Experiments were performed in the absence of extracellular HCO_3^-/CO_2 and Na$^+$ (bars) on ducts stimulated with secretin (1 nM). *A*, example of pH$_i$ measurement in a duct subjected to an ammonium pulse and 0 Na$^+$ during the first 5 min of recovery. Subsequently, the same maneuver was done and also K$^+$ was removed. After the cations were restored to the buffer, the normal pH$_i$ response to the ammonium pulse was obtained. The *bottom* figures show the summary of the data for this protocol. *B*, comparison of pH$_i$ recovery from ammonium induced acidosis during control conditions without Na$^+$ (0 Na$^+$), and when ouabain (3 mM) was added to the bathing solution. Addition of ouabain completely abolished or even reversed the pH$_i$ recovery, The top graph shows the original recording, and the bottom is the summary of data. Experiments were performed in the absence of extracellular HCO_3^-, and ducts were stimulated with secretin.

the non-gastric type H$^+$-K$^+$-ATPase. In our hands a short-term removal of extracellular K$^+$ eliminated pH$_i$ recovery, and the effect was fully reversible. Similarly, the pH$_i$ recovery was abolished with ouabain (Fig. 6*B*), which is known to block the non-gastric H$^+$-K$^+$ pump (11, 17). That is, addition of ouabain (3 mM) stopped the pH$_i$ recovery and this effect was fully reversible. Addition of ouabain or removal of K$^+$ for short time periods is not likely to run-down cell ion gradients, which was demonstrated earlier by microelectrode recordings in duct cells (4).

Taken together, pH$_i$ experiments reveal that pancreatic ducts have very robust pH$_i$ regulation and a redundancy of H$^+$/HCO$_3^-$ transporters, including the gastric and non-gastric H$^+$-K$^+$ pumps. These transporters can contribute to pH$_i$ regulation and/or net transepithelial H$^+$/HCO$_3^-$ transport. By "experimentally removing" some of the transporters, it was possible for the first time to demonstrate functional gastric and non-gastric H$^+$-K$^+$ pumps in pancreatic ducts. Now the task was to see whether pancreatic duct epithelium expressed such H$^+$-K$^+$ pumps and whether they could contribute to secretion.

Expression of Gastric and Non-gastric H$^+$-K$^+$ Pumps—We examined expression of gastric and non-gastric pump α-sub-
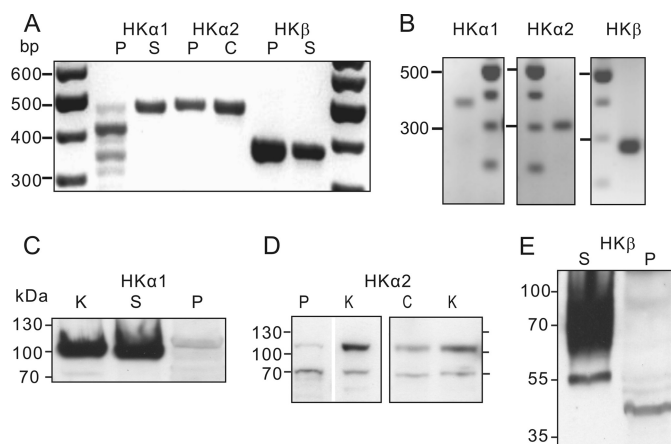

FIGURE 7. **Expression of gastric and non-gastric H$^+$-K$^+$ pumps.** *A*, RT-PCR on mRNA extracted from whole rat pancreas (*P*), stomach (*S*), or colon (*C*). Samples were run with primers for α-subunits of the gastric H$^+$-K$^+$ pump (HKα1), non-gastric H$^+$-K$^+$ pump (HKα2) and β-subunit for the gastric H$^+$-K$^+$ pump (HKβ). The expected transcripts were 476, 486, and 373 bp, respectively. *B*, nested PCR on single isolated pancreatic ducts showing transcripts for HKα1, HKα2, and HKβ subunits. The expected transcripts were 350, 307, and 276 bp, respectively. Purity of duct preparations was checked (see "Experimental Procedures"). Primer sets are given in Table 1. Identity of all products was confirmed by sequencing. *C–E*, Western blot on membrane fraction proteins extracted and from pancreas (*P*), stomach (*S*), kidney (*K*), and colon (*C*). *C*, gastric H$^+$-K$^+$ antibody (Calbiochem 119101) was used. *D*, non-gastric antibody HKα2 antibody (C384-M79) (17) was used. *E*, antibody directed against gastric HKβ (Sigma A2749) was used. See supplemental Figs. S1–3 for controls.

TABLE 1
Primers used for rat RT-PCR and nested PCR

Primer sets	Size
Rat tissue RT-PCR primers	
rHKstomach forward: 5′-ACC CTC CCC GGG CCA CCG T-3′	476 bp
rHKstomach reverse: 5′-CAG CAA GAT CAT GTC AGC AGC A-3′	
rHKcolon forward: 5′-TCC ATG ATC GAC CCT CCT CGG T-3′	485 bp
rHKcolon reverse: 5′-TAG TAA GAC CAT GTC AGC TGC G-3′	
rHKβ forward: 5′-CTT CGA CAA CCC CCA CGA CCC-3′	372 bp
rHKβ reverse: 5′-AGG ACA GAC AAA TGG TCA CAG-3′	
Rat tissue nested PCR primers	
rHKstomachnest forward: 5′-CGT TCC AGA TGC TGT GCT CAA-3′	350 bp
rHKstomachnest reverse: 5′-TTA CAG CCA CAA TGG CAC CC-3′	
rHKcolonnest forward: 5′-GTG CCA GAC GCA GTC TCC AAA T-3′	307 bp
rHKcolonnest reverse: 5′-TGA TCA ACT TCT GCT GGG GTG A-3′	
rHKβnest forward: 5′-CCC TAT GAA GGG AAG GTG GAG T-3′	276 bp
rHKβnest reverse: 5′-GTG TTA ACC GCA CGG GAT TG-3′	

units, and also β-subunit of the gastric pump. Methods were optimized for the labile pancreas preparations and we used colon, stomach and kidney as controls. RT-PCR analysis on whole rat pancreas shows that there are transcripts for α-subunit and β-subunit of the gastric H$^+$-K$^+$ pump, as well as α-subunit for the non-gastric pump (Fig. 7*A*). See Table 1 for primers. To pinpoint whether mRNA is indeed originating from pancreatic ducts, single ducts were collected and PCR was run with nested primers (Fig. 7*B*). Notably, the data on pure ducts also show the expression of the H$^+$-K$^+$ pump subunits. Protein expression was also detected by Western blot analysis on α-subunits of both gastric and non-gastric pumps (Fig. 7, *C* and *D*). Control experiments are shown in the supplemental Figs. S1–S3. Note that two bands were observed with the HKα2 antibody in the kidney, colon, and more variably in pancreas. These could correspond to the known full-length HKα2a and an N-terminal-truncated variant HKα2b (29). There are discrepancies regarding the enzyme activity of
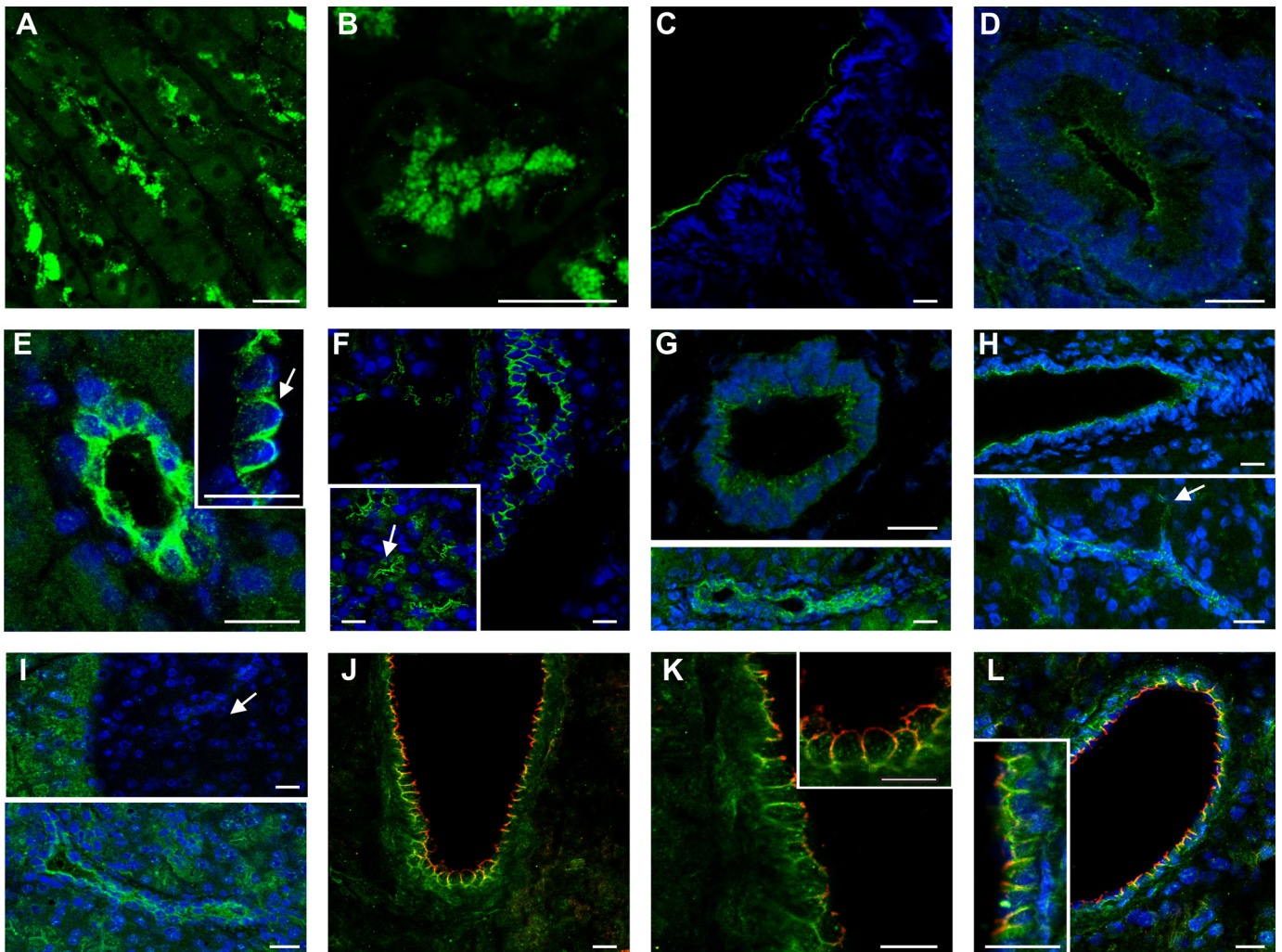
FIGURE 8. **Localization of H^+-K^+ pumps in stomach (A, B), colon (C, D), and rat pancreas (E–L).** A and B, stomach, longitudinal, and transverse images of gastric pits and close-up of tubulovesiscles labeled for gastric H^+-K^+ pump with anti-HKα1 AB 1679 antibody and Alexa 488 (*green*). C and D, colonic pits in longitudinal and transverse cuts labeled with non-gastric HKα2 antibody (C384-M79), Alexa 488 and nuclear stain DAPI (*blue*). E. Images of pancreatic duct labeled with N-terminal gastric anti-HKα1 AB 1679, Alexa488, and DAPI; *arrow* on the *inset* shows lumen. F, same antibody showing different sizes of dilated intralobular and intercallated ducts (*arrows*); images are from pancreas stimulated with secretin. G, images of pancreas labeled with C-terminal gastric HKα1 antibody (119101), Alexa488 and DAPI. H, pancreas labeled with monoclonal HKα1 antibody (119100), Alexa488, and DAPI shows labeling of intralobular ducts and centroacinar cells (*arrow*). I, pancreas labeled with non-gastric HKα2 antibody (C384-M79), Alexa488, and DAPI. Islet of Langerhans (*arrow*) only label with nuclear stain. J–L, colocalization of the gastric H^+-K^+ pump (119100 antibody and *red* Cy3) and non-gastric H^+-K^+ pump (C384-M79 antibody and *green* Alexa488), with and without DAPI; *insets* show close up duct cells. Images F and L were taken from pancreas stimulated with secretin. All bars are 20 μm, and images are taken from 10 independent immunohistochemical experiments. See supplemental Fig. S4 for controls.

the truncated variant (17, 29). We also probed samples for the gastric β-subunit (Fig. 7E). The expected band size for the core protein is 35 kDa, and the fully glycosylated protein from the stomach is 60–90 kDa. In pancreas we detect a 40 kDa band.

Our study is the first study on pancreas where both types of H^+-K^+ pump α-subunits and the β-subunit have been detected on both mRNA and protein levels. Although either type of analysis on pancreas have been attempted before, no consistent results were obtained, most likely due to powerful pancreatic proteases and nucleotidases (30, 31).

Using immunofluorescence and confocal microscopy we localized the H^+-K^+ pumps in rat pancreas preparations. We used several antibodies against α-subunits, and in addition stomach (Fig. 8, A and B) and colon (Fig. 8, C and D) served as positive controls. Other controls are shown in the supplemental Fig. S4. In pancreas the fluorescence of the gastric pump was detected in or close to plasma membranes in unstimulated and secretin-stimulated pancreas. Using three different antibodies, the gastric H^+-K^+ pump fluorescence was localized to both luminal and lateral membrane areas of small and larger intralobular and interlobular pancreatic ducts (Fig. 8, E–H). In addition, the pump was detected in intercalated ducts (Fig. 8, F and H) and in luminal aspects of pancreatic acini, which are lined with small and flat centro-acinar cells thought to be of ductal lineage. The non-gastric H^+-K^+ pump fluorescence was also detected in similar locations along the duct (Fig. 8I). In colocalization experiments we show that the gastric and non-gastric pump distribution overlaps on lateral membranes, and the gastric pump was more prominent on the luminal membranes (Fig. 8, J–L). In pancreas pre-stimulated with secretin (Fig. 8, F and L), the H^+-K^+ pumps seem
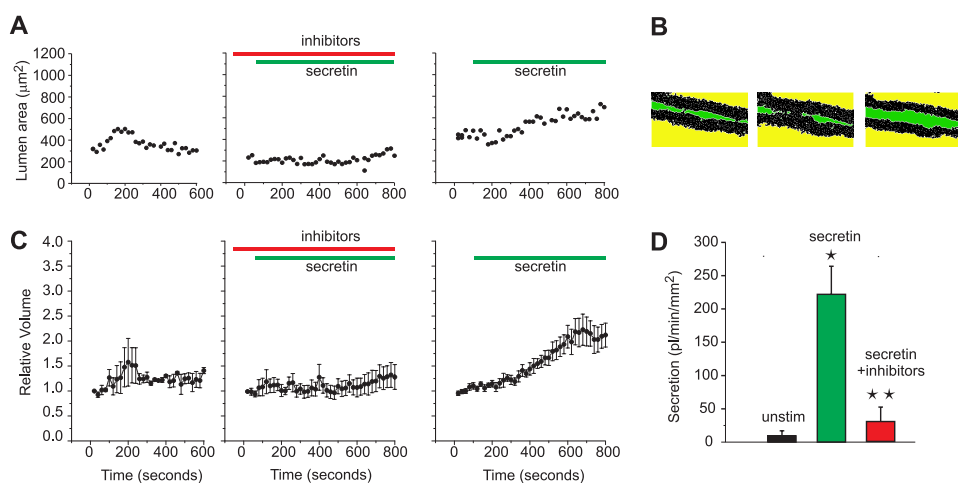
FIGURE 9. **Effect of H⁺-K⁺ pump inhibitors on secretion in isolated ducts.** *A*, luminal area of a single duct shown as a function of time: without stimulation; stimulated with secretin; and with secretin and omeprazol plus SCH-28080. For concentrations see Fig. 3. *B*, example of a duct 107 μm in length. The fluorescence of Dextran Texas Red was used do delineate the duct and images shown here are converted single binary images used for analysis in the three corresponding conditions. *C*, relative volumes of same ducts in three experimental conditions (means $\pm$ S.E., $n = 7$). *D*, secretory rates, corrected for initial area of the duct epithelium, are given for unstimulated and secretin-stimulated ducts with and without pump inhibitors. Secretin stimulated secretion significantly (*), and the H⁺-K⁺ pump inhibitors decreased the secretin-stimulated secretion by 86% (**).

to have similar overall distribution as in the non-stimulated tissue.

Secretion in Isolated Ducts Is Inhibited by H⁺-K⁺ Pump Inhibitors—The key question is whether H⁺-K⁺ pumps contribute to ductal secretion? We set up a new fluorescence-based method using Dextran Texas Red to measure secretion in freshly prepared single intra-lobular and intercalated pancreatic ducts. Secretin evoked secretion, seen in single images as increase in lumen area (Fig. 9, *A* and *B*). Omeprazole and SCH-28080 clearly prevented significant part of the secretin effect in the same duct. Luminal area values can be converted to relative volumes and secretion rates per epithelial surface area by making some simple assumptions (Fig. 9*C*) (see "Experimental Procedures"). Following these, we can deduce that secretin evokes secretion of 220 pl/min/mm² of epithelium (Fig. 9*D*). This value is probably an underestimate of the real secretion, as the ducts were not fully occluded and some had small branches. Nevertheless, the values are comparable to those obtained in larger intra- and interlobular from the rodent ducts that were cultured and sealed (32, 33). Most important, the H⁺-K⁺ pump inhibitors reduced secretion by 85%. These secretion experiments were done in the presence of physiological solutions (containing extracellular Na⁺ and HCO₃⁻), which shows that indeed the pumps contributed significantly to secretion, not only to a fraction of pH$_i$ regulation as revealed in the extreme experimental conditions necessary for pH experiments (Figs. 5 and 6).

DISCUSSION

We have shown that rat pancreatic ducts express gastric and non-gastric H⁺-K⁺ pumps. It may seem somewhat surprising that the HCO₃⁻-secreting epithelium expresses H⁺-K⁺ pumps, but functional pH$_i$ and secretion studies indicate that the proton pumps may be important in pancreatic duct physiology. Here we argue how.

First of all, H⁺-K⁺ pumps contribute to secretin-stimulated secretion in small pancreatic ducts. Using new imaging meth-

ods, we show for the first time that small ducts (intercalated and intralobular) secrete rather large quantities of fluid in physiological conditions. Most importantly, inhibition of the H⁺-K⁺ pump alone was more effective in decreasing secretion compared with inhibition of either NHE, NBC, or AE (32, 34). One explanation is that the pump inhibitors hit the primary, active, and regulated transcellular H⁺/HCO₃⁻ transport. The other transporters that rely on Cl⁻ or Na⁺ gradients are responsible for the pH$_i$ regulation. Indeed the pH$_i$ regulation is very robust in duct cells and there is a redundancy of H⁺/HCO₃⁻ transporters that defend it. That is, if one/two transporters are inhibited, the remaining transporter can maintain pH$_i$ recovery following the ammonium pulse challenge. Therefore, contribution from these transporters (NHE, NBC, and AE) had to be "experimentally removed" before the contribution of the H⁺-K⁺ pumps on pH$_i$ were uncovered. In general terms, measurements of intracellular pH, or for that matter Ca²⁺, indicate transport of H⁺/HCO₃⁻/Ca²⁺ and Ca²⁺ signaling, but these may not always reflect the integrated event of secretion. Subsequently, as the second line of evidence for the pumps, we could demonstrate pH$_i$ sensitivity to omeprazol as well as to SCH-28080, low K⁺ and ouabain, indicating the gastric and non-gastric pumps, respectively.

The third line of evidence is that for the first time expression of both types of H⁺-K⁺ pump α-subunits and the β-subunit on both mRNA and protein levels is shown for pancreas. Although either type of analysis on pancreas have been attempted before, no consistent results were obtained, most likely due to powerful pancreatic proteases and nucleotidases (30, 31). We have tried to combat these problems by optimizing our methods. The β-subunit deserves an extra mention. There are 6–7 *N*-glycosylation sites on the extracellular domain of the β-subunit and they are important for the assembly, maturation, and sorting of the enzyme (35). The lower size of the subunit detected in pancreas indicates either deg-

radation by pancreatic enzymes during preparation, or actual lower degree of glycosylation. If the latter is the case, we cannot be sure that the luminal H$^+$-K$^+$ pump is inserted properly and functional (see below).

This leads us to a discussion of the pump localization. The immunohistochemical data indicate that the both the gastric and non-gastric H$^+$-K$^+$ α-subunits localize to the lateral membranes and the luminal membranes of various ducts. How does that compare with other epithelia? For the kidney it is accepted that the gastric H$^+$-K$^+$ pump is constitutively expressed on the apical membrane of distal tubuli (9, 14). Immunolocalization studies on the cortical collecting ducts show the pump on the luminal membranes of α-type intercalated cells, and also on the basolateral membrane of β-type cells (36) and in cytoplasm (37). The non-gastric H$^+$-K$^+$ pump is localized on apical membranes of surface cells of the distal colon and the anterior prostate (38–40). Heterologous expression studies on kidney cells show that the non-gastric pump expressed together with the gastric β-subunit localizes to the luminal membrane of the MDCK cells but to the lateral membrane of the LLC-PK1 cells (41). It seems that the short extracellular loop between T3 and T4 region is critical for the pump delivery and a single mutation can redirect the pump from the apical to the basolateral site (42). On the whole, such studies show that assembly and polarized distribution of pumps is complex and depends on the glycosylated β-subunits, as well as on specific sorting motifs of the α-subunit and other associating proteins (13, 43).

Returning back to the pancreatic ducts, the H$^+$-K$^+$ pump localized on the lateral membrane would be sufficient to explain the functional data (see below). Here also β1-subunit of the Na$^+$,K$^+$-ATPase would be available for the assembly. The localization of a functional pump to the luminal membrane is not certain, firstly because of the poorly-glycosylated β-subunit. Secondly, one should be cautious about immunofluorescence images, as they do not reveal whether the protein is correctly inserted into the membrane (42). Nevertheless, as unusual as it may seem, there are other native epithelia secreting bicarbonate, such as the insect midgut and fish intestine, that express proton pumps (vacuolar-type H$^+$ pump) on the luminal membranes and their role in regulation of bicarbonate secretion is puzzling (44, 45). Similarly, the function of H$^+$-K$^+$ pumps, if correctly inserted into the luminal membrane of pancreatic ducts, is at present not clear.

For the following discussion, we will assume that the lateral H$^+$-K$^+$ pumps are functional and analyze whether they could be a major factor in HCO$_3^-$ transport, and whether this could drive fluid secretion. Let us do some enabling calculations using the pH$_i$ recovery rates. We determined that in the Na$^+$-free and HCO$_3^-$-free conditions, when the H$^+$-K$^+$ pump was detected, dpH/dt was 0.09, and calculated flux $J(H^+)$ lies between 7 and 13 mM/minute, depending on the variable buffering power in a pH$_i$ range 6.2 to 6.8 (Fig. 4). The intact rat pancreas stimulated with secretin secretes about 5 μl/minute per gram tissue weight, and ducts make at most 4% of the tissue volume in rat pancreas. Thus, if ducts were solely responsible for this secretion, they could secrete some 190 μl/minute per ml of cell water volume. If then $J(H^+)$ results in $J(HCO_3^-)$ se-
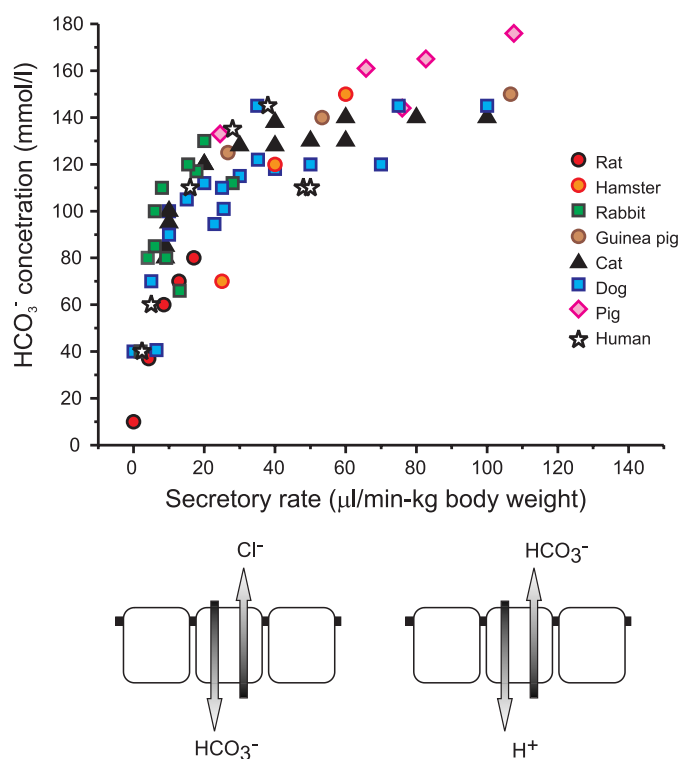

FIGURE 10. **The relation between secretory rate and HCO$_3^-$ concentration for pancreatic juice collected from pancreas of various species.** Secretion was stimulated with secretin and secretory rates are corrected for body weight. The data for rat, hamster, rabbit, cat, dog, pig, and human were taken from publications and recalculated (46, 54–62). The figure also shows schematic duct cells: to the right is a cell from small ducts of any species that following stimulation secretes HCO$_3^-$/absorbs H$^+$, total secretion rates depend on a number of such ducts; to the left is a cell from larger/interlobular ducts that secretes Cl$^-$ and/or exchanges HCO$_3^-$ for Cl$^-$, processes that are most apparent at low secretory rates.

cretion, this can contain between 37 and 68 mM HCO$_3^-$. Most likely, in normal conditions, *i.e.* in a CO$_2$/HCO$_3^-$ buffer, where H$^+$ is provided by the carbonic anhydrase, the H$^+$-K$^+$-ATPase could account for much greater HCO$_3^-$ flux. If we take that under these conditions $J(H^+)$ or $J(HCO_3^-)$ is about 40 mM/minute, as we measured (Fig. 2), ducts can theoretically secrete up to 200 mM HCO$_3^-$. Thus, intralobular rat pancreatic ducts have the H$^+$-K$^+$-ATPase that has a capacity to contribute to formation of a HCO$_3^-$-rich secretion.

We still have one problem to solve regarding the relatively low HCO$_3^-$ concentrations in rat pancreatic juice (at the most containing 80 mM HCO$_3^-$ and with pH values lower than 8) as compared with the concentrations in the so called high HCO$_3^-$ secretors, such as man, where HCO$_3^-$ concentrations are 100–150 mM and pH values are above 8 (3). The simplest explanation is as follows. Consider the classical textbook figure of the relation between secretory rates and HCO$_3^-$ concentration of pancreatic juice. Here we compile the figure (Fig. 10) for different animals, where pancreas was stimulated with secretin, and importantly, we correct secretion for the body weight and assume proportionality to the gland weight. It is striking that all curves follow the same pattern. Firstly, at high secretory rates stimulated ductal HCO$_3^-$ secretion dominates, and as we suggest from the data in the present study, this process may involve the H$^+$-K$^+$-ATPase presumably lo-
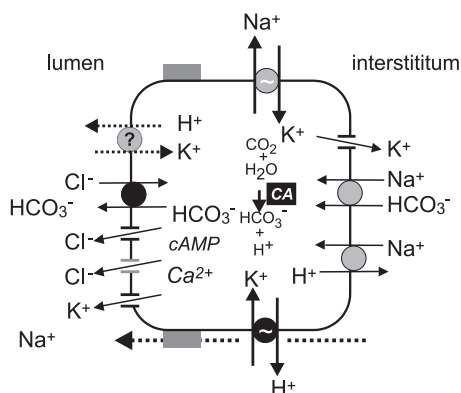
FIGURE 11. **Cellular model for pancreatic HCO_3^- secretion.** The classical model (1, 2) is extended with other ion transporters and channels reviewed in Refs. 3, 63. The molecular identities may be as follows: Cl^- channels (CFTR and TMEM16A), K^+ channels (IK and BK), Na^+/H^+ transporter (NHE1), Na^+-1–2HCO_3^- cotransporter (pNBC1), and Cl^-/2HCO_3^- exchanger (SLC26A6), carbonic anhydrase (CA). The present study shows evidence for the H^+-K^+ pumps, which together with key transport partners (*black*) can support secretion.

cated on the basolateral membranes of small pancreatic ducts (Fig. 11). Secondly, at low secretory rates modification of this secretion becomes important and HCO_3^- decreases, while Cl^- increases. For example, HCO_3^- secretion could be diluted by a concurrent Cl^- secretion originating from acini or larger intra- and interlobular ducts (1, 32). Alternatively, modification of the primary HCO_3^--rich secretion could occur in downstream larger ducts, which have been shown to perform HCO_3^- "salvaging", or simply HCO_3^-/Cl^- exchange (46, 47), and they express a number of transporters that would enable this function (3). Furthermore, the present study indicates luminal H^+-K^+ pumps, and if functional, they could contribute to this process by H^+ secretion. Ductal modification of secretion also occurs in other exocrine glands, such as salivary ducts and sweat ducts.

The apparent difference between so called high HCO_3^- secretors (such as man, dog, and cat) and low HCO_3^- secretors (such as rat and mouse) may simply relate to the number of "secretory" ducts, not necessarily to different secretory mechanisms. Indeed, morphological studies show that duct system is not well developed in rat pancreas, where it contributes only 2–4% of pancreas volume, while in cat, dog and human the ductal system is well developed, and in human pancreas ducts contribute 14–25% of pancreas volume (48–50).

The above arguments would indicate that "a duct is not a duct". Small ducts, intralobular, intercalated and also centroacinar cells (probably duct-like), are rich in carbonic anhydrase, CFTR (25–27) and as this study also shows, the H^+-K^+ pumps. Furthermore, as we show the pH_i recovery rates in small rat pancreatic ducts are very high in the normal Na^+- and HCO_3^--repleted state, at least ten times higher than that in the larger ducts (most likely larger intralobular and interlobular) obtained from the pig, guinea pig, and mouse pancreas and in human duct cell lines (6, 33, 51). Thus, high pH_i recovery rates and secretion rates indicate that we are dealing with the most active secretory ducts in our study.

In conclusion, the finding that rat pancreas expresses both the gastric and non-gastric H^+-K^+ pumps with some overlap in localization indicates that they must be part of a robust functional system, that is, they contribute significantly to secretion in pancreatic ducts. We envisage that there is an inverse mechanism to that functioning in parietal cells of the stomach. Namely, in pancreas H^+ is pumped into interstitium and HCO_3^- is left in the lumen. We argue that the H^+-K^+ pumps may be a unifying mechanism for HCO_3^--driven secretion in pancreas in general. The future challenge is to integrate the H^+-K^+ pump with other H^+/HCO_3^- transporters (that may have primary function in pH_i regulation) and with CFTR and K^+ channels (Fig. 11). Furthermore, we need to understand whether the H^+-K^+ pump functions on both the luminal and basolateral membranes and division of labor between the gastric and non-gastric H^+-K^+ type. In addition, heterogeneity of structure and function of a pancreatic ductal tree requires dedicated studies. Pancreatic duct secretion has a central role in whole pancreas physiology. Therefore, as the function of pancreatic ducts is disturbed in cystic fibrosis, pancreatitis, and pancreatic cancer, it is of relevance to understand the role of H^+-K^+ pumps in pancreatic pathophysiology. Moreover, as proton pump inhibitors are very widely used in westernized countries (52, 53), one should re-evaluate their effect and role in pancreatic and gastrointestinal diseases.

REFERENCES

1. Novak, I., and Greger, R. (1988) *Pflügers Arch.* **411,** 546–553
2. Gray, M. A., Greenwell, J. R., and Argent, B. E. (1988) *J. Membr. Biol.* **105,** 131–142
3. Steward, M. C., Ishiguro, H., and Case, R. M. (2005) *Annu. Rev. Physiol.* **67,** 377–409
4. Novak, I., and Greger, R. (1988) *Pflügers Arch.* **411,** 58–68
5. de Ondarza, J., and Hootman, S. R. (1997) *Am. J. Physiol.* **272,** G124–G134
6. Villanger, O., Veel, T., and Raeder, M. G. (1995) *Gastroenterology* **108,** 850–859
7. Zhao, H., Star, R. A., and Muallem, S. (1994) *J. Gen. Physiol.* **104,** 57–85
8. Codina, J., Delmas-Mata, J. T., and Dubose, T. D., Jr. (1998) *J. Biol. Chem.* **273,** 7894–7899
9. Jaisser, F., and Beggah, A. T. (1999) *Am. J. Physiol.* **276,** F812–F824
10. Dunbar, L. A., and Caplan, M. J. (2001) *J. Biol. Chem.* **276,** 29617–29620
11. Grishin, A. V., Bevensee, M. O., Modyanov, N. N., Rajendran, V., Boron, W. F., and Caplan, M. J. (1996) *Am. J. Physiol.* **271,** F539–F551
12. Crambert, G., Horisberger, J. D., Modyanov, N. N., and Geering, K. (2002) *Am. J. Physiol. Cell Physiol.* **283,** C305–C314
13. Caplan, M. J. (2007) *J. Clin. Gastoenterol.* **41,** S217–S221
14. Silver, R. B., and Soleimani, M. (1999) *Am. J. Physiol.* **276,** F799–F811
15. Shibata, T., Hibino, H., Doi, K., Suzuki, T., Hisa, Y., and Kurachi, Y. (2006) *Am. J. Physiol. Cell Physiol.* **291,** C1038–C1048
16. Pestov, N. B., Korneenko, T. V., Shakhparonov, M. I., Shull, G. E., and Modyanov, N. N. (2006) *Am. J. Physiol. Cell Physiol.* **291,** C366–C374
17. Swarts, H. G., Koenderink, J. B., Willems, P. H., and De Pont, J. J. (2005) *J. Biol. Chem.* **280,** 33115–33122
18. Hede, S. E., Amstrup, J., Christoffersen, B. C., and Novak, I. (1999) *J. Biol. Chem.* **274,** 31784–31791
19. Githens, S., 3rd, Holmquist, D. R., Whelan, J. F., and Ruby, J. R. (1980) *J. Cell Biol.* **85,** 122–135

20. Novak, I., and Greger, R. (1991) *Pflügers Arch.* **419,** 76–83
21. Novak, I., and Christoffersen, B. C. (2001) *Pflügers Arch.* **441,** 761–771
22. Li, D., Ren, W., Wang, X., Wang, F., Gao, Y., Ning, Q., Han, Y., Song, T., and Lu, S. (2009) *Appl. Biochem. Biotechnol.* **158,** 253–261
23. Haanes, K. A., and Novak, I. (2010) *Biochem. J.* **429,** 303–311
24. Sørensen, C. E., Amstrup, J., Rasmussen, H. N., Ankorina-Stark, I., and Novak, I. (2003) *J. Physiol.* **551,** 881–892
25. Hyde, K., Reid, C. J., Tebbutt, S. J., Weide, L., Hollingsworth, M. A., and Harris, A. (1997) *Gastroenterology* **113,** 914–919
26. Kumpulainen, T., and Jalovaara, P. (1981) *Gastroenterology* **80,** 796–799
27. Marino, C. R., Matovcik, L. M., Gorelick, F. S., and Cohn, J. A. (1991) *J. Clin. Invest.* **88,** 712–716
28. Burghardt, B., Elkaer, M. L., Kwon, T. H., Rácz, G. Z., Varga, G., Steward, M. C., and Nielsen, S. (2003) *Gut* **52,** 1008–1016
29. Kone, B. C., and Higham, S. C. (1998) *J. Biol. Chem.* **273,** 2543–2552
30. Pestov, N. B., Romanova, L. G., Korneenko, T. V., Egorov, M. V., Kostina, M. B., Sverdlov, V. E., Askari, A., Shakhparonov, M. I., and Modyanov, N. N. (1998) *FEBS Lett.* **440,** 320–324
31. Herrmann, M., Selige, J., Raffael, S., Sachs, G., Brambilla, A., and Klein, T. (2007) *Scand. J. Gastroenterol.* **42,** 1275–1288
32. Fernández-Salazar, M. P., Pascua, P., Calvo, J. J., López, M. A., Case, R. M., Steward, M. C., and San Román, J. I. (2004) *J. Physiol.* **556,** 415–428
33. Szalmay, G., Varga, G., Kajiyama, F., Yang, X. S., Lang, T. F., Case, R. M., and Steward, M. C. (2001) *J. Physiol.* **535,** 795–807
34. Ishiguro, H., Naruse, S., Steward, M. C., Kitagawa, M., Ko, S. B., Hayakawa, T., and Case, R. M. (1998) *J. Physiol.* **511,** 407–422
35. Sachs, G., Shin, J. M., Vagin, O., Lambrecht, N., Yakubov, I., and Munson, K. (2007) *J. Clin. Gastroenterol.* **41,** Suppl. 2, S226–S242
36. Bastani, B. (1995) *J. Am. Soc. Nephrol.* **5,** 1476–1482
37. Kraut, J. A., Helander, K. G., Helander, H. F., Iroezi, N. D., Marcus, E. A., and Sachs, G. (2001) *Am. J. Physiol. Renal Physiol.* **281,** F763–F768
38. Lee, J., Rajendran, V. M., Mann, A. S., Kashgarian, M., and Binder, H. J. (1995) *J. Clin. Invest.* **96,** 2002–2008
39. Rajendran, V. M., Singh, S. K., Geibel, J., and Binder, H. J. (1998) *Am. J. Physiol.* **274,** G424–G429
40. Pestov, N. B., Korneenko, T. V., Adams, G., Tillekeratne, M., Shakhparonov, M. I., and Modyanov, N. N. (2002) *Am. J. Physiol. Cell Physiol.* **282,** C907–C916
41. Reinhardt, J., Grishin, A. V., Oberleithner, H., and Caplan, M. J. (2000) *Am. J. Physiol. Renal Physiol.* **279,** F417–F425
42. Lerner, M., Lemke, D., Bertram, H., Schillers, H., Oberleithner, H., Caplan, M. J., and Reinhardt, J. (2006) *Cell Physiol. Biochem.* **18,** 75–84
43. Dunbar, L. A., Aronson, P., and Caplan, M. J. (2000) *J. Cell Biol.* **148,** 769–778
44. Wieczorek, H., Beyenbach, K. W., Huss, M., and Vitavska, O. (2009) *J. Exp. Biol.* **212,** 1611–1619
45. Wood, C. M., Bucking, C., and Grosell, M. (2010) *J. Exp. Biol.* **213,** 2681–2692
46. Case, R. M., Harper, A. A., and Scratcherd, T. (1969) *J. Physiol.* **201,** 335–348
47. Lee, M. G., Ahn, W., Choi, J. Y., Luo, X., Seo, J. T., Schultheis, P. J., Shull, G. E., Kim, K. H., and Muallem, S. (2000) *J. Clin. Invest.* **105,** 1651–1658
48. Bouwens, L., and Pipeleers, D. G. (1998) *Diabetologia* **41,** 629–633
49. Githens, S. (1988) *J. Pediatr. Gastroenterol. Nutr.* **7,** 486–506
50. Kodama, T. (1983) *Acta Pathol. Jpn.* **33,** 297–321
51. Shumaker, H., Amlal, H., Frizzell, R., Ulrich, C. D., 2nd, and Soleimani, M. (1999) *Am. J. Physiol.* **276,** C16–C25
52. Lee, J. K., and Enns, R. (2007) *World J. Gastroenterol.* **13,** 6296–6313
53. Shaheen, N. J., Hansen, R. A., Morgan, D. R., Gangarosa, L. M., Ringel, Y., Thiny, M. T., Russo, M. W., and Sandler, R. S. (2006) *Am. J. Gastroenterol.* **101,** 2128–2138
54. Sewell, W. A., and Young, J. A. (1975) *J. Physiol.* **252,** 379–396
55. Ali, A. E., Rutishauser, S. C., and Case, R. M. (1990) *Pancreas* **5,** 314–322
56. Seow, K. T., Case, R. M., and Young, J. A. (1991) *Pancreas* **6,** 385–391
57. Padfield, P. J., Garner, A., and Case, R. M. (1989) *Pancreas* **4,** 204–209
58. Case, R. M., Harper, A. A., and Scratcherd, T. (1968) *J. Physiol.* **196,** 133–149
59. Bro-Rasmussen, F., Killmann, S. A., and Thaysen, J. H. (1956) *Acta Physiol. Scand.* **37,** 97–113
60. Chey, W. Y., Kim, M. S., and Lee, K. Y. (1979) *J. Physiol.* **293,** 435–446
61. Grotmol, T., Buanes, T., Mathisen, O., Schistad, O., Sejersted, O. M., and Raeder, M. G. (1985) *Acta Physiol. Scand.* **124,** 71–80
62. Domschke, S., Domschke, W., Rösch, W., Konturek, S. J., Wünsch, E., and Demling, L. (1976) *Gastroenterology* **70,** 533–536
63. Novak, I. (2008) *Purinergic Signal.* **4,** 237–253